Available online at www.sciencedirect.com

ScienceDirect

Journal of the European Ceramic Society 29 (2009) 691–696

www.elsevier.com/locate/jeurceramsoc

Porous zirconium titanate ceramics synthesized by sol–gel process

J. Macan [a,*], A. Gajović [b], H. Ivanković [a]

[a] *University of Zagreb, Faculty of Chemical Engineering and Technology, Marulićev trg 19, P.O. Box 177, HR-10000 Zagreb, Croatia*
[b] *Ruđer Bošković Institute, Materials Physics Department, Molecular Physics Laboratory, Bijenička 54, P.O. Box 180, HR-10002 Zagreb, Croatia*

Received 25 March 2008; received in revised form 4 July 2008; accepted 9 July 2008
Available online 20 August 2008

Abstract

Zirconium titanate, $ZrTiO_4$, was synthesized by sol–gel method from zirconium butoxide and titanium isopropoxide. Amorphous $ZrTiO_4$ powder was ground, calcined at 500 °C, and milled to homogenize size distribution of the powder. Milled powder was pressed into tablets and sintered at 900–1400 °C for 8 h. Differential scanning calorimetry and dilatometric studies indicated crystallization of $ZrTiO_4$ at 600–700 °C. Raman spectroscopy and X-ray diffraction analysis confirmed presence of crystallized $ZrTiO_4$ already at 900 °C, and crystallite size was determined by Scherrer equation. Scanning electron microscopy showed that $ZrTiO_4$ grains begin to sinter at higher temperatures, starting from 1200 °C, while preserving high porosity up to 1300 °C as confirmed by dilatometry and mercury intrusion porosimetry.
© 2008 Elsevier Ltd. All rights reserved.

Keywords: Sol–gel processes; Sintering; Porosity; Zirconium titanate

1. Introduction

Zirconium titanate, $ZrTiO_4$, is a ceramic material with very good thermal and electrical properties and high resistance to heat and corrosive environment. These properties lead to its widespread use in electronic components for telecommunication purposes, such as condensers and resonators.[1] ZrO_2–TiO_2 mixed oxides are also used as catalysts,[2,3] and lately applicability of $ZrTiO_4$ for humidity sensors is also being investigated.[4] High purity and homogeneity of ceramic material is essential for all these applications. This is difficult to achieve by classical procedure of sintering a stoichiometric mixture of zirconia (ZrO_2) and titania (TiO_2) powders at temperatures up to 1600 °C for several days.[1,5] High-energy milling of ZrO_2 and TiO_2 which reduces crystallite size to give almost amorphous powders can lower the transition temperature as low as 1100 °C.[6–8] But this approach is also energy costly, and attrition of milling balls can increase content of impurities.[6,8] Because of this, sol–gel process is increasingly used to prepare homogeneous and amorphous $ZrTiO_4$ powder which crystallizes at temperatures several hundred degrees lower than in previous methods. $ZrTiO_4$ can be prepared by hydrolysis and condensation reactions of inorganic salts[3,9–11] or alkoxides.[2,12–14] Ceramics synthesized by sol–gel process are also very pure and their microstructure is comparatively easy to tailor.[15]

Previous research of $ZrTiO_4$ ceramics sintered from powder prepared by high-energy ball milling of ZrO_2 and TiO_2 has shown that electrical conductivity in humid air is highly dependant on porosity.[16] High porosity combined with mechanical stability is also desirable for catalysts. In this work $ZrTiO_4$ amorphous powder was prepared by sol–gel process from zirconium and titanium alkoxides, pressed into tablets and sintered at different temperatures. The influence of temperature on crystallization, sintering behaviour and microstructure of prepared $ZrTiO_4$ ceramics was studied.

2. Experimental

2.1. Preparation and characterisation of amorphous $ZrTiO_4$ powder

Zirconium titanate, $ZrTiO_4$, was synthesized by sol–gel method from zirconium butoxide ($Zr(C_4H_9O)_4$, 80%, Fluka) and titanium isopropoxide ($Ti(C_3H_7O)_4$, 97%, Aldrich), stabilised with 0.3 mol of acetylacetone ($C_5H_8O_2$, Fluka) per mole of alkoxide, in 2-propanol solution. Stabilised alkoxides were hydrolysed with stoichiometric amount of water for full

---

* Corresponding author. Tel.: +385 1 4597 226; fax: +385 1 4597 250.
E-mail address: jmacan@pierre.fkit.hr (J. Macan).

0955-2219/$ – see front matter © 2008 Elsevier Ltd. All rights reserved.
doi:10.1016/j.jeurceramsoc.2008.07.001

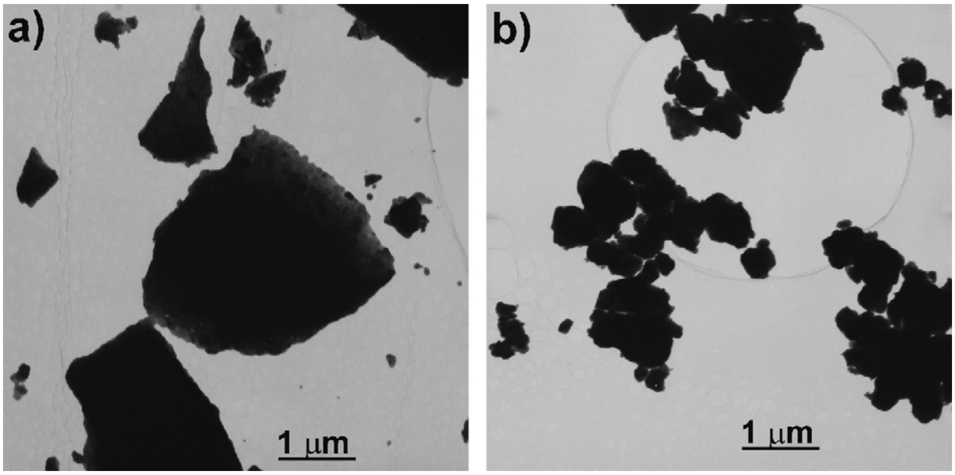

Fig. 1. Transmission electron micrographs of (a) unmilled and (b) milled amorphous $ZrTiO_4$ powder calcined at 500 °C.

condensation of alkoxides (2 moles/mole of alkoxide), added as 4.64 mol/dm^3 nitric acid that served as catalyst. Transparent sol was left to gel at room temperature. The resulting gel was dried at 110 °C, ground and sieved to remove particles larger than 80 μm, calcined at 500 °C to remove residual organic content, and milled. Milling was performed for 2 h in air using a Fritsch planetary ball mill Pulverisette 6 with vial and balls of 94% zirconia, with rotation speed of 500 rpm and powder-to-ball weight ratio of 1:10.

Specific surface area of milled and unmilled powder, previously degassed overnight at 250 °C, was determined by inverse BET method from nitrogen adsorption–desorption isotherms at liquid N_2 temperature on a Micromeritics ASAP 2000, from measurements at 5 relative nitrogen pressures in 0.05–0.21 range. Amorphous powders were observed by transmission electron microscopy (TEM) and checked by selected area electron diffraction (SAED) on microscope JEOL JEM-200CX with tungsten cathode operating at accelerating voltage of 200 kV. Thermal behaviour of the milled powder was studied by simultaneous differential scanning calorimetry and thermogravimetric

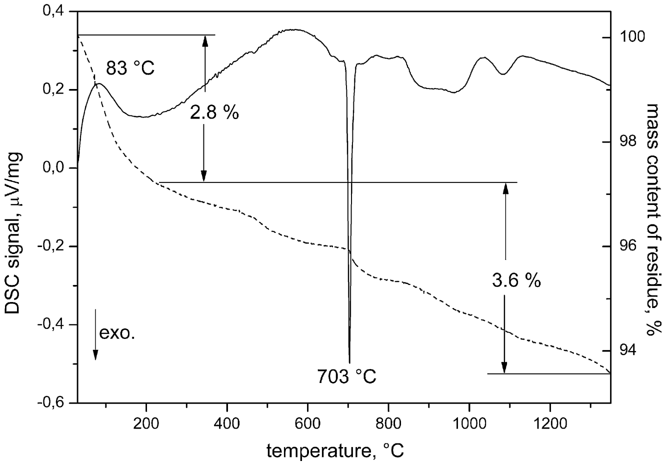

Fig. 2. Combined differential scanning calorimetry and thermogravimetric analysis of $ZrTiO_4$ amorphous powder calcined at 500 °C, performed in air at 10 °C/min.

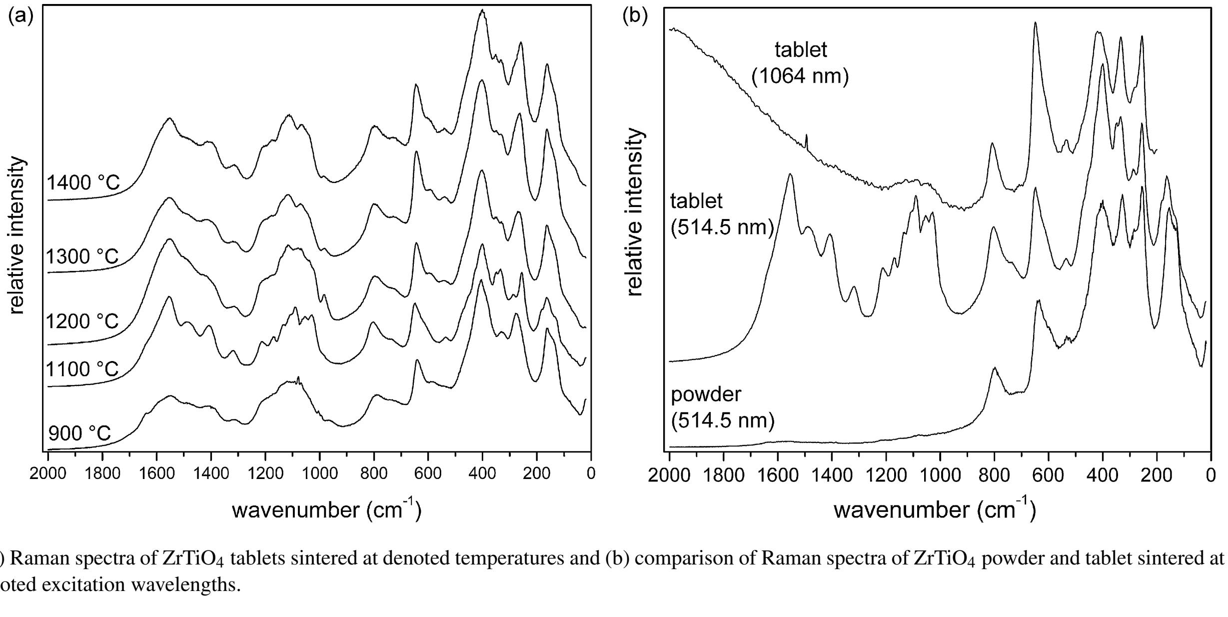

Fig. 3. (a) Raman spectra of $ZrTiO_4$ tablets sintered at denoted temperatures and (b) comparison of Raman spectra of $ZrTiO_4$ powder and tablet sintered at 1100 °C, using denoted excitation wavelengths.

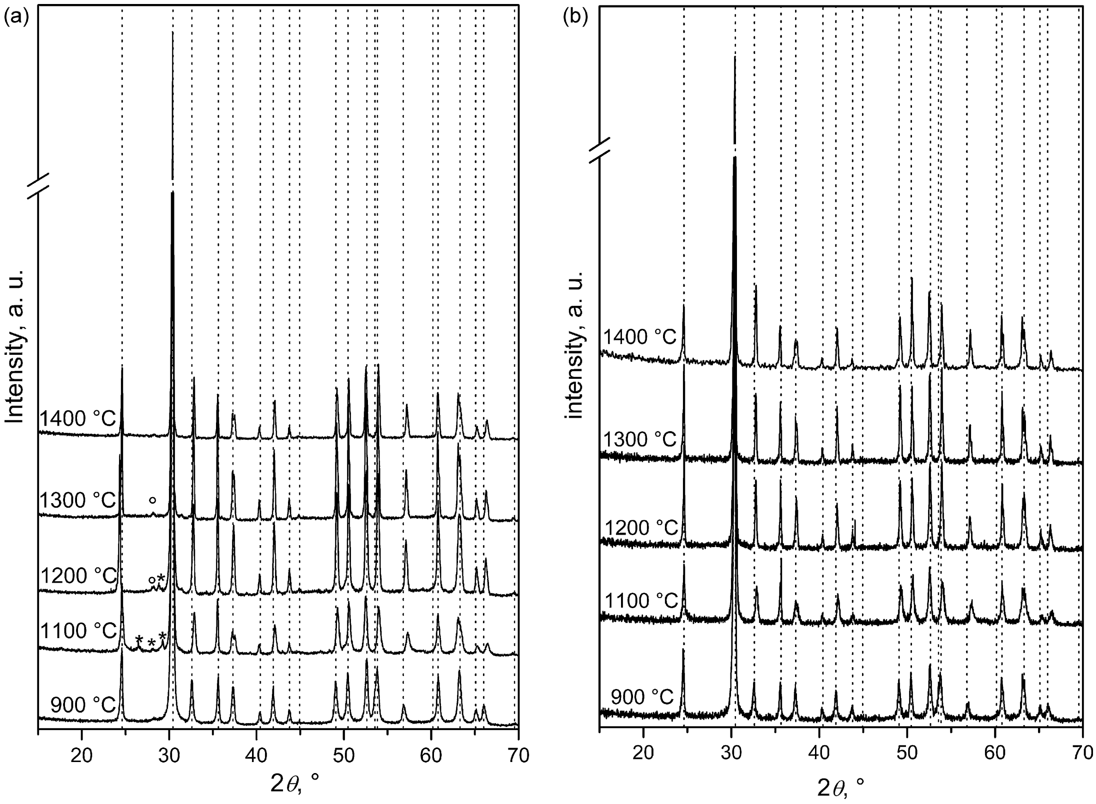

Fig. 4. X-ray diffractograms of (a) $ZrTiO_4$ tablets and (b) $ZrTiO_4$ powder sintered at denoted temperatures; JCPDS data for zirconium titanate (34-415) shown as dotted lines, Ti_9O_{17} (71-631) marked with * and $Zr_{0.944}O_2$ (81-1314) marked with °.

analysis (DSC–TGA) on a Netzsch thermoanalyzer STA 409. Sample was heated from room temperature to 1350 °C at a heating rate of 10 °C/min in a synthetic air flow of 30 cm^3/min.

2.2. Preparation and characterisation of sintered $ZrTiO_4$ ceramics

Milled powder was uniaxially pressed (180 MPa) into tablets and sintered for 8 h in a muffle furnace with Pt–PtRh thermocouple at 900, 1100, 1200, 1300 and 1400 °C. Furnace was heated to sintering temperature at 23 °C/min. For comparison, unpressed calcined powder was sintered in same conditions.

Raman spectroscopy measurements were performed using DILOR Z24 triple monochromator with Coherent Innova 400 argon ion laser operating at 514.5 nm for excitation, applied laser power was 150 mW. To reduce the heating of the sample during measurement, the incident laser beam was focused in the line shape. To distinguish possible luminescence, additional experiment was performed using FT-Raman PerkinElmer System 2000 spectrometer, with 1064 nm excitation. X-ray powder diffraction (XRD) analysis was performed on Phillips PW 1820 instrument using Cu Kα radiation with a scanning rate of 0.12°/min. Crystallite size was determined using Scherrer equation, taking fully crystallized rutile, TiO_2, as a standard.

Thermodilatometric study was carried out on uniaxially pressed (250 MPa) compacts (10 mm × 3 mm × 3 mm) using horizontal loading differential dilatometer Netzsch DIL 402ED operating at 5 °C/min heating rate. Porosity of the sintered tablets was measured using Carlo Erba Mercury Intrusion Porosimeter 2000 WS, on samples weighing approximately 1 g in pressure range 0–2000 atm. Scanning electron microscopy (SEM) of sintered samples, previously gold-coated, was performed on JEOL T300 microscope operating at 25 kV.

3. Results and discussion

Milling of amorphous powder homogenizes the size distribution, as can be seen from TEM micrographs (Fig. 1), but

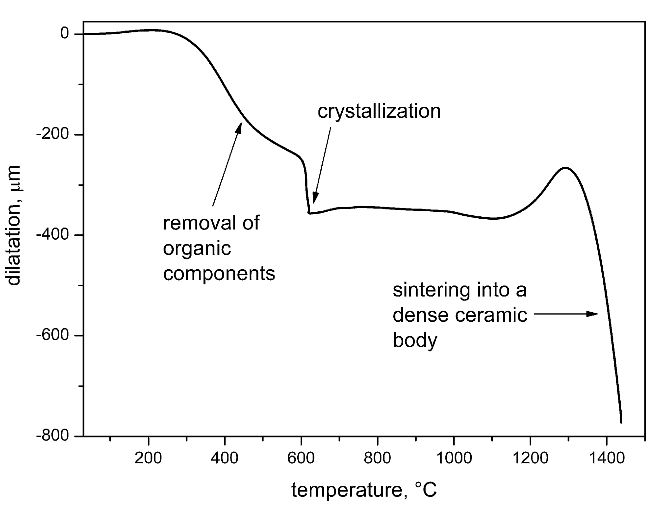

Fig. 5. Dilatometric curve of amorphous 10 mm long compact heated at 5 °C/min.

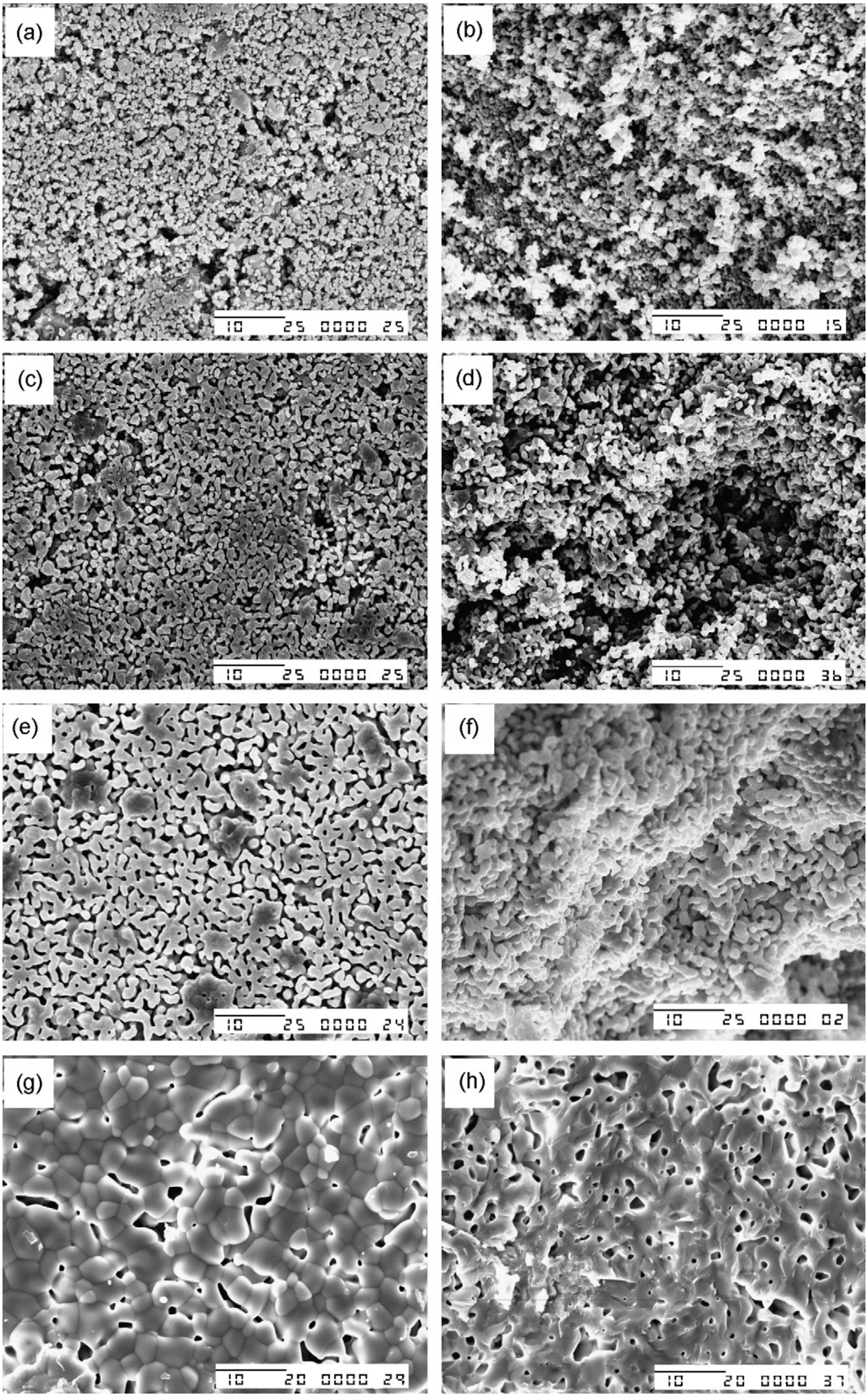

Fig. 6. SEM micrographs of surfaces and insides of tablets sintered at 1100 °C (a and b), 1200 °C (c and d), 1300 °C (e and f) and 1400 °C (g and h); scale bar is 10 μm.

also causes agglomeration and decreases specific surface to 12.2 m^2/g, compared with 83.2 m^2/g of unmilled powder. Average particle size of milled powder as determined from TEM is in the 0.25–1 μm range, and milled powder remained fully amorphous as confirmed by SAED. The milled powder was chosen for further investigation to ensure homogeneous particle size distribution.

Results of DSC–TGA analysis are given in Fig. 2. The first mass loss evident on the TGA curve and accompanied by a DSC endothermic maximum at 83 °C is due to evaporation of adsorbed water. The mass loss decreases approximately constantly with further temperature increase, which is ascribed to slow degradation of residual organic content. Large DSC exothermic maximum at 703 °C is due to crystallization of amorphous $ZrTiO_4$, as confirmed by our preliminary research. Raman spectroscopy (Fig. 3) and XRD analysis (Fig. 4) confirm that samples sintered at 900 °C and higher temperatures are crystalline $ZrTiO_4$.

$ZrTiO_4$ with orthorhombic symmetry (space group *Pbcn*) and two formula units in a unit cell has 33 optically active modes of vibration, 18 of which are Raman active. Only $ZrTiO_4$ bands were observed in 20–900 cm^{-1} region of the Raman spectra of sintered tablets (Fig. 3a). The bands for all the samples are broad, which can be attributed to random distribution of Zr^{4+} and Ti^{4+} ions in equivalent sites of crystal lattice, oxide defects and nonstoichiometric variations of Zr/Ti ratio in polycrystalline ceramics.[17,18] Number of resolved Raman bands varies with sintering time, indicating differences in structural order.[17] In the Raman spectrum of the sample sintered at 1100 °C, 12 out of 18 expected $ZrTiO_4$ bands were resolved: 132, 160, 256, 286, 332, 404, 468 (shoulder), 536, 588 (shoulder), 640, 730 and 804 cm^{-1}. It should be noted that the bands at 256 and 286 cm^{-1} were resolved only in the sample sintered at 1100 °C, while the band at 588 appeared only as a shoulder. A band at 350 cm^{-1} that does not belong to $ZrTiO_4$ was observed in the Raman spectra of all sintered ceramics. This band could be an indicator of some nonstochiometry, since the most intensive band of $Zr_5Ti_7O_{24}$ exists in the vicinity of this position.[17] Additional intensive part of spectra was detected at wavenumbers higher than 1000 cm^{-1}. These additional bands do not appear in unpressed powdered samples calcined in the same conditions, while this part of spectrum changes completely when different laser excitation was used (Fig. 3b). This is an indicator of luminescence origin of the bands. De Lucena et al.[19] show that $ZrTiO_4$ displays broad band photoluminescence with the maximum around 560 nm, caused by a change in coordination number of titanium and zirconium. Since we observed luminescence at absolute wavenumber of ~17,900 cm^{-1} (~559 nm), it could be caused by electronic transition between new electronic states possibly formed due to oxygen defects inside the pores of the ceramic bodies. Moreover, mass loss evident from TGA curve (Fig. 2) indicates continued degradation of residual organic components at higher temperatures, so the content of available oxygen inside the pores would decrease causing the oxygen defects. Further investigation of this effect is planned.

XRD measurements confirm that all sintered ceramics crystallize in orthorhombic symmetry, as indicated in Fig. 4 by dotted JCPDS data lines for zirconium titanate (34-415). Tablets sintered at 1100–1300 °C contain minute amounts of Ti_9O_{17} (71-631, marked with *) and $Zr_{0.944}O_2$ (81-1314, marked with °), which do not appear in powders sintered at those temperatures. Development of these phases may be a consequence of local inhomogeneities in composition of the tablets due to phase separation caused by pressing. Increase in sintering temperature promotes crystallite growth, which is apparent from decreased width and increased intensity of XRD maxima. Average crystallite size in tablets and unpressed powders was determined by Scherrer equation from broadening of the XRD maxima (Table 1), using TiO_2 sintered at 1200 °C as a standard to correct for the instrumental broadening. The strain contribution to the broadening could be neglected in the calculation at low Bragg angles.[20] The apparent crystallite size expectedly increases with sintering temperature both in tablets and in unpressed powders. The increase is smaller in tablets, presumably because the crystallite growth in compacted tablets is slowed due to encounter with grain boundaries of neighbouring crystallites.

Table 1
Crystallite size as determined by Scherrer equation and porosity as determined by mercury intrusion, for $ZrTiO_4$ powders and tablets sintered at listed temperatures

Temperature (°C)	Crystallite size (nm)		Porosity (%)
	Tablets	Powders	
900	30	35	47.5
1100	40	40	48.9
1200	55	90	42.1
1300	95	130	48.3
1400	115	130	21.4

Dilatometric curve (Fig. 5) shows that, after initial shrinking due to removal of organic components, sample suddenly shrinks at 614 °C. This corresponds to crystallization of $ZrTiO_4$, shifted to lower temperature than in DSC curve due to slower heating rate. Additional shrinking after 1300 °C is caused by sintering of porous $ZrTiO_4$ into a dense ceramic body. This is confirmed by porosimetry measurements (Table 1) and SEM micrographs of surfaces and insides of tablets (Fig. 6). SEM micrographs also show grain growth with increased temperature of sintering. It can be seen that grains start to sinter together at 1200 °C and still retain very high porosity up to at least 1300 °C. Increased temperature of sintering also increases mechanical strength of tablets: while tablets sintered at 900 °C crush easily, those fired at 1200 and 1300 °C are much more resilient in spite of their high porosity. Therefore, sol–gel process shows potential for preparation of porous $ZrTiO_4$ ceramic bodies.

4. Conclusions

The ceramic bodies were prepared by sintering of the amorphous powder, which was prepared by sol–gel process and milled to homogenize particle size distribution to 0.25–1 μm. Amorphous powder crystallizes at 600–700 °C, depending on heating rate. Porosity of the ceramic bodies can be tailored by changing the sintering temperature. Samples do not start to lose their porosity until temperatures higher than 1300 °C. It is therefore possible to prepare fully crystallized porous $ZrTiO_4$ ceramic in this manner.

Acknowledgments

Authors would like to thank the Ministry of Science, Education and Sport of the Republic of Croatia for the financial support of this study, which is a part of research projects "Bioceramic, Polymer and Composite Nanostructured Materials", 125-1252970-3005 and "Physics and applications of nanostructures and bulk matter", 098-0982904-2898. The authors would also like to thank Mr. J. Schmauch, University of Saarland, Germany, for performing thermodilatometric analysis, Dr. G. Matijašić, University of Zagreb, Croatia, for BET measurements, and Dr. V. Mohaček-Grošev, Ruđer Bošković Institute, Croatia, for FT-Raman measurements and relevant discussion.

References

1. Park, Y., Kim, Y. H. and Kim, H. G., The phase transition and microwave dielectric properties of tin modified zirconium titanate by melting process. *Mater. Sci. Eng. B*, 1996, **40**, 37–41.
2. Barrera, M. C., Viniegra, M., Escobar, J., Vrinat, M., de los Reyes, J. A., Murrieta, F. and García, J., Highly active MoS_2 on wide-pore ZrO_2–TiO_2 mixed oxides. *Catal. Today*, 2004, **98**, 131–139.
3. Fung, J. and Wang, I., Dehydrocyclization of C_6–C_8 *n*-paraffins to aromatics over TiO_2–ZrO_2 catalysts. *J. Catal.*, 1991, **130**, 577–587.
4. Cosentino, I. C., Muccillo, E. N. S. and Muccillo, R., Development of zirconia–titania porous ceramics for humidity sensors. *Sens. Actuators B*, 2003, **96**, 677–683.
5. McHale, A. E. and Roth, R. S., Low-temperature phase relationships in the system ZrO_2–TiO_2. *J. Am. Ceram. Soc.*, 1986, **69**, 827–832.
6. Stubičar, M., Bermanec, V., Stubičar, N., Kudrnovski, D. and Krumes, D., Microstructure evolution of an equimolar powder mixture of ZrO_2–TiO_2 during high-energy ball-milling and post-annealing. *J. Alloys Compd.*, 2001, **316**, 316–320.
7. Gajović, A., Furić, K., Musić, S., Djerdj, I., Tonejc, A., Tonejc, A. M., Su, D. S. and Schlögl, R., Mechanism of $ZrTiO_4$ synthesis by mechanochemical processing of TiO_2 and ZrO_2. *J. Am. Ceram. Soc.*, 2006, **89**, 2196–2205.
8. Gajović, A., Djerdj, I., Furić, K., Schlögl, R. and Su, D. S., Preparation of nanostructured $ZrTiO_4$ by solid state reaction in equimolar mixture of TiO_2 and ZrO_2. *Cryst. Res. Technol.*, 2006, **41**, 1076–1081.
9. Karakchiev, L. G., Zima, T. M. and Lyakhov, N. Z., Low-temperature synthesis of zirconium titanate. *Inorg. Mater.*, 2001, **37**, 386–390.
10. Lu, Q. F., Chen, D. R. and Jiao, X. L., Synthesis of long $ZrTiO_4$ fibers by a sol–gel process free of organic components. *J. Mater. Chem.*, 2003, **13**, 1127–1131.
11. Zhang, S. X., Li, J. B., Cao, J., Zhaim, H. Z. and Zhang, B., Preparation, microstructure and microwave dielectric properties of $Zr_xTi_{1-x}O_4$ ($x = 0.40$–0.60) ceramics. *J. Eur. Ceram. Soc.*, 2001, **21**, 2931–2936.
12. Sham, E. L., Aranda, M. A. G., Farfan-Torres, E. M., Gottifredi, J. C., Martínez-Lara, M. and Bruque, S., Zirconium titanate from sol–gel synthesis—thermal decomposition and quantitative phase analysis. *J. Solid State Chem.*, 1998, **139**, 225–232.
13. de Farias, R. F. and Airoldi, C., Spherical particles of zirconia–titania of hexagonal structure from a neutral amine route. *J. Colloid Interface Sci.*, 1999, **220**, 255–259.
14. Naci Koç, S., Zirconium titanate synthesis by diethanol amine based sol–gel route. *J. Sol–Gel Sci. Technol.*, 2006, **38**, 277–281.
15. Jones, R. W., *Fundamental Principles of Sol–Gel Technology*. The Institute of Metals, London, 1989.
16. Ličina, V., Gajović, A., Moguš-Milanković, A., Djerdj, I., Tomašić, N. and Su, D. S., Correlation between the microstructure and the electrical properties of $ZrTiO_4$ ceramics. *J. Am. Ceram. Soc.*, 2008, **91**, 178–186.
17. Azough, F., Freer, R. and Petzelt, J., A Raman spectral characterization of ceramics in the system ZrO_2–TiO_2. *J. Mater. Sci.*, 1993, **28**, 2273–2276.
18. Krebs, M. A. and Condrate Sr., R. A., A Raman spectral characterization of various crystalline mixtures in ZrO_2–TiO_2 and HfO_2–TiO_2 systems. *J. Mater. Sci. Lett.*, 1988, **7**, 1327–1330.
19. de Lucena, P. R., Leite, E. R., Pontes, F. M., Longo, E., Pizani, P. S. and Varela, J. A., Photoluminescence: a probe for short, medium and long-range self-organization order in $ZrTiO_4$ oxide. *J. Solid State Chem.*, 2006, **179**, 3997–4002.
20. Klug, H. P. and Alexander, L. E., *X-ray Diffraction Procedures*. J. Wiley, New York, 1974.